# Terahertz frequency comb by multifrequency-heterodyning photoconductive detection for high-accuracy, high-resolution terahertz spectroscopy

Takeshi Yasui,[a] Yasuhiro Kabetani, Eisuke Saneyoshi, Shuko Yokoyama, and Tsutomu Araki
*Graduate School of Engineering Science, Osaka University, 1-3 Machikaneyama, Toyonaka, Osaka 560-8531, Japan*

(Received 1 February 2006; accepted 20 April 2006; published online 13 June 2006)

We report a terahertz spectroscopy technique based on a stable terahertz frequency comb from a photoconductive terahertz emitter driven by a stabilized femtosecond laser. To this end, a photocurrent frequency comb is induced in a photoconductive terahertz detector by instantaneous photogating with another detuned femtosecond laser and is applied to read out the terahertz frequency comb. The detailed structure of the terahertz frequency comb was clearly observed with frequency accuracy of $2.5\times10^{-7}$ and resolution of 81.8 MHz using multifrequency-heterodyning photoconductive detection, which in turn is caused by the slightly mismatched frequency spacing between terahertz and photocurrent frequency combs. © *2006 American Institute of Physics*. [DOI: 10.1063/1.2209718]

A femtosecond mode-locked laser generates a sequence of pulses that are essentially copies of the same pulse separated by an interval equal to the inverse of the mode-locked frequency. The highly stable femtosecond mode-locked pulse train is synthesized by a series of frequency spikes regularly separated by the mode-locked frequency in the optical frequency domain. This structure is referred to as a frequency comb. Since the frequency-comb structure can be used as a precision ruler in the frequency domain, the femtosecond-laser-based optical frequency comb has received a lot of interest as a powerful metrological tool capable of covering the visible to near-infrared region by virtue of precise laser stabilization and the use of microstructured photonic crystal fiber.[1] Recently, the concept of the frequency comb has been extended to the mid-infrared region by using a femtosecond laser in combination with the nonlinear difference frequency generation process,[2] and effectively applied to a frequency-comb-based Fourier-transform infrared spectrometer (comb-FTIR) based on a multifrequency-heterodyning interferometric technique.[3,4] Furthermore, a possibility to extend comb-FTIR to the terahertz region is discussed. On the other hand, a terahertz electromagnetic pulse, radiating from a photoconductive antenna or nonlinear optical crystal triggered by a femtosecond laser, is also composed of a regular comb of sharp lines in the terahertz frequency domain. This so-called terahertz frequency comb possesses attractive features for high-precision terahertz spectroscopy, namely, excellent accuracy and stability, broadband selectivity, ultranarrow linewidth, and exact multiplication. Furthermore, since the terahertz frequency comb is extended to the terahertz region without any frequency offset, it is possible to achieve absolute calibration without the use of a standard laser or a standard material. Thus the terahertz frequency comb is suitable for identifying molecules of interest with fingerprints in the terahertz region, including gas molecules,[5] illicit drugs,[6] biological molecules,[7] and explosives.[8] There are, however, no reports of femtosecond-laser-based terahertz frequency comb although terahertz spectroscopy based on electronic frequency-comb technique has been reported.[9] In this letter, we propose femtosecond-laser-based terahertz frequency-comb spectroscopy using multifrequency-heterodyning photoconductive detection.

Let us consider terahertz generation from a photoconductive emitter excited by a femtosecond laser (pump laser; mode-locked frequency=$f_1$) and terahertz detection using a photoconductive detector gated by another femtosecond laser (probe laser; mode-locked frequency=$f_2$). Figure 1 illustrates spectral behaviors in (a) optical, (b) terahertz, and (c) radio-frequency (rf) regions. In the frequency domain, since the photoconductive generation of the terahertz pulse can be considered as an ultrawideband demodulation of an optical frequency comb, the frequency comb is downconverted to the terahertz region without any change to the frequency spacing. The resulting terahertz frequency comb is a har-

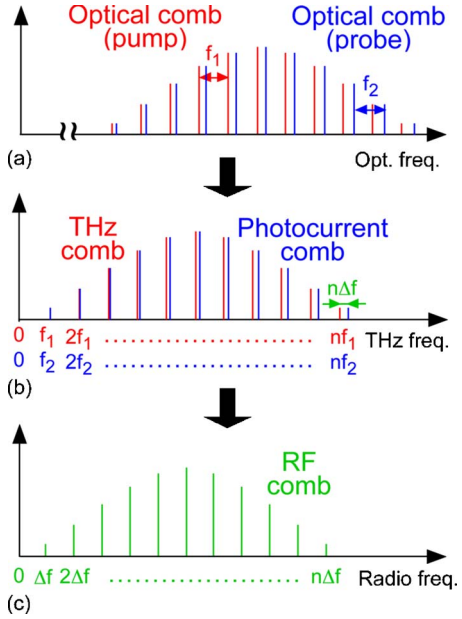


FIG. 1. Spectral behavior of frequency combs in (a) optical, (b) terahertz, and (c) rf regions.

[a]Electronic mail: t-yasui@me.es.osaka-u.ac.jp

 

monic frequency comb without a frequency offset, composed of a fundamental component (frequency=$f_1$) and a series of harmonic components (frequency=$2f_1, 3f_1, \ldots, nf_1$) of a mode-locked frequency. Next, we consider what happens when the mode-locked frequency of the probe laser ($f_2=f_1+\Delta f$) is slightly detuned from that of the pump laser ($f_1$) by a certain frequency offset ($\Delta f$). Instantaneous photoconductive gating by the probe laser induces a photocurrent frequency comb having a different frequency spacing [frequency=$f_2, 2f_2, 3f_2, \ldots$, $nf_2=(f_1+\Delta f), 2(f_1+\Delta f), 3(f_1+\Delta f), \ldots, n(f_1+\Delta f)$] in the photoconductive detector, which also exists in terahertz frequency region. Under this condition, it is possible to detect the terahertz pulse as a result of the photoconductive process occurring between the terahertz and photocurrent frequency combs, giving rise to the multifrequency-heterodyning effect. This results in the generation of a secondary frequency comb in the rf region, termed the rf comb (frequency=$\Delta f, 2\Delta f, 3\Delta f, \ldots, n\Delta f$). Since the rf comb is a replica of the terahertz frequency comb only downscaled by $f_1/\Delta f$ in frequency, one can utilize the terahertz frequency comb easily via direct observation of the rf comb using a rf spectrum analyzer and calibration of the frequency scale.

To confirm the above concept, we used two Kerr-lens mode-locked Ti:sapphire lasers as a pump laser and a probe laser. The individual mode-locked frequencies in the two lasers ($f_1$ and $f_2$) and the frequency difference between them ($\Delta f=f_1-f_2$) were stabilized by two independent laser-control systems composed of phase-locked loop (PLL) and a piezoelectric transducer (PZT) attached to a laser mirror. In PLL electronics, the 100th harmonic component of a mode-locked frequency ($100f_1$ and $100f_2$) and a synthesized signal from a rubidium frequency standard (accuracy=$5\times10^{-11}$, stability=$2\times10^{-11}$ at 1 s) are used as a control signal and a reference signal, respectively. The resulting $f_1$ and $f_2$ are fixed at 81 800 000 and 81 800 100 Hz within a range of $\pm1.6\times10^{-3}$ Hz whereas the fluctuation of $\Delta f$ is suppressed within $\pm2.5\times10^{-5}$ Hz at a gate time of 1 s. Such excellent stability of $f_1$, $f_2$, and $\Delta f$ enables us to generate stable frequency combs and achieve an exact multifrequency-heterodyning process. We first used two bowtie-shaped, low-temperature-grown GaAs photoconductive antennas (bowtie length=1 mm, gap=5 $\mu$m) as a terahertz emitter and a terahertz detector. The terahertz frequency comb radiated from the terahertz emitter propagated in free space and then was incident onto the terahertz detector via two hemispherical silicon lenses and two off-axis parabolic mirrors. As a result of multifrequency-heterodyning photoconductive detection, the rf comb was directly measured with a rf spectrum analyzer (Agilent Technologies, E4402B) after passing through a current preamplifier (sensitivity=$4\times10^6$ V/A, bandwidth=1 MHz). One can reconstruct the terahertz frequency comb exactly by calibrating the rf comb with the frequency downscale factor (=$f_1/\Delta f$=818 000).

Figure 2(a) shows an amplitude spectrum of the rf comb obtained using the proposed method (measurement time=10 s, resolution bandwidth=10 kHz), in which the upper horizontal axis gives the frequency scale in the rf spectrum analyzer. The spectrum was obtained by subtracting a background spectrum measured in the absence of the terahertz electric field from a signal spectrum. The actual frequency values in the terahertz frequency-comb spectrum are scaled according to the lower horizontal axis by using the frequency downscale factor. Considering a spectral range of 0.3 THz and a frequency spacing of 81.8 MHz, the terahertz spectrum is composed of 3667 comb modes. The inset of Fig. 2(a) shows an expansion of the spectral region of 0.0492–0.0498 THz (measurement time=0.5 s, resolution bandwidth=10 Hz). One can clearly see seven comb-mode lines having a frequency spacing of 81.8 MHz and a width of 11 MHz; these can be used as divisions in a terahertz frequency-comb ruler with a frequency resolution of 81.8 MHz. The accuracy of the observed terahertz frequency comb is determined by stability of frequency spacing and frequency downscale factor. We can conclude the accuracy in the proposed terahertz-comb spectroscopy to be $2.5\times10^{-7}$ from stability of $f_1$ [=$(1.6\times10^{-3})/81\,800\,000=2.0\times10^{-11}$] and that of $\Delta f$ [=$(2.5\times10^{-5})/100=2.5\times10^{-7}$]. As usual, the accuracy in conventional terahertz time-domain spectroscopy (THz-TDS) using a mechanical time-delay stage is determined by precision of step displacement (=$\sim10^{-2}$ in a motor-driven stage). In contrast to it, the accuracy in the present system depends on stability of frequency spacing and frequency downscale factor, resulting in achievement of excellent accuracy. In Fig. 2(a), the spectral bandwidth is limited by employing two bowtie-shaped photoconductive antennas as a terahertz emitter and detector. Next, to extend the spectral bandwidth over 1 THz, we use a dipole-shaped photoconductive antenna (length=7.5 $\mu$m, width=10 $\mu$m, gap=5 $\mu$m) as a terahertz detector and magnify the frequency downscale factor to 16 360 000 by changing the $\Delta f$ value of 100 to 5 Hz in combination with another high-gain current

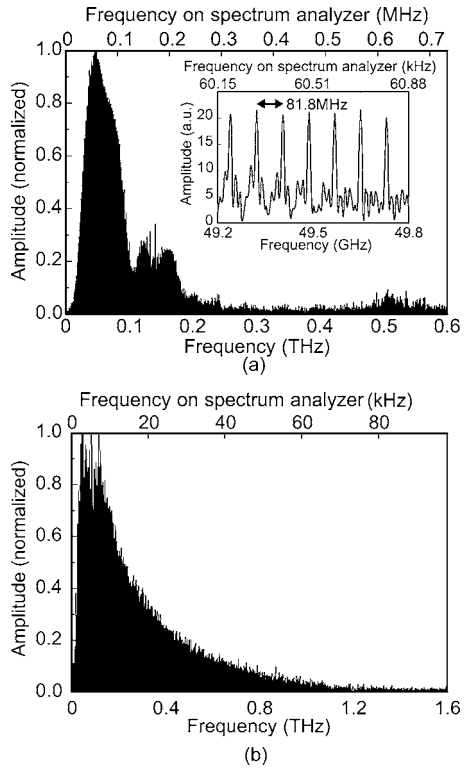


FIG. 2. Amplitude spectrum of terahertz frequency comb obtained with multifrequency-heterodyning photoconductive detection. (a) Bowtie-photoconductive terahertz emitter and bowtie-photoconductive terahertz detector and (b) bowtie-photoconductive terahertz emitter and dipole-photoconductive terahertz detector are used. An enlarged terahertz-comb spectrum is also shown as an inset. Frequency scale in terahertz and rf combs is indicated at lower and upper horizontal coordinates, respectively.

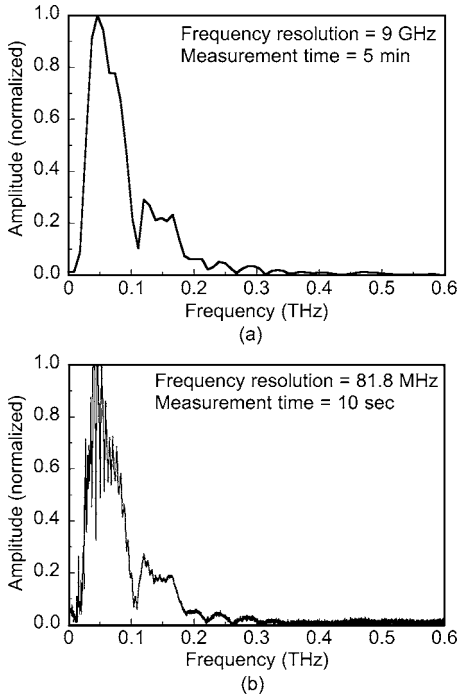


FIG. 3. Terahertz amplitude spectra obtained with (a) stage-scanning THz-TDS and (b) AOS-THz-TDS. Bowtie-photoconductive terahertz emitter and bowtie-photoconductive terahertz detector are used.

preamplifier (sensitivity $=5\times10^7$ V/A, bandwidth $=100$ kHz). The resulting spectrum is shown in Fig. 2(b) (measurement time $=1000$ s, resolution bandwidth $=1$ kHz). One can clearly confirm that the amplitude spectrum of terahertz frequency comb is extended over 1 THz.

To evaluate the validity of the terahertz frequency-comb spectrum shown in Fig. 2(a), we compare the resultant spectrum with those obtained by stage-scanning THz-TDS and asynchronous optical sampling THz-TDS (AOS-THz-TDS).[10,11] The AOS-THz-TDS enables a stage-free configuration in THz-TDS and hence achieves ultrahigh spectral resolution with rapid data acquisition. Figures 3(a) and 3(b) show the terahertz spectra obtained with stage-scanning THz-TDS and AOS-THz-TDS, respectively. The frequency resolutions in the former and latter are 9 GHz at a measurement time of 5 min and 81.8 MHz at a measurement time of 10 s, respectively. The spectral structure in Fig. 3(b) is due to multiple reflection of the terahertz pulse in the hemispherical silicon lens. After comparing the terahertz amplitude spectra obtained using the three methods, we can conclude that the proposed method correctly measures the terahertz amplitude spectrum. The proposed terahertz-comb spectroscopy and AOS-THz-TDS achieve the theoretical limit of frequency resolution in THz-TDS, namely, mode-locked frequency, at a shorter measurement time. However, the terahertz-comb spectroscopy provides a few attractive features compared with AOS-THz-TDS. The AOS-THz-TDS needs an additional sum-frequency-generation (SFG) cross-correlator to generate a trigger signal as a time origin for time-domain measurement and hence provide phase spectrum of terahertz radiation. Furthermore, even if the measurement time is much shorter for AOS-THz-TDS, one usually has to perform fast Fourier transformation (FFT) on a computer in order to obtain the terahertz spectrum of amplitude after making the measurement. In contrast to AOS-THz-TDS, the proposed terahertz-comb spectroscopy can measure the terahertz amplitude spectrum directly without a SFG cross-correlator, similar to comb-FTIR,[3,4] and FFT because it is an entirely frequency-domain measurement, which also means that it does not require time coincidence or time-delay scanning between the terahertz and probe pulses. These features of terahertz-comb spectroscopy enable rapid data analysis and a simple, stable setup in high-accuracy, high-resolution terahertz spectroscopy.

This work was supported by the SCOPE from MIC of Japan, the ITRGP2002 from NEDO of Japan, and KAKE-HHI No. 1868600 from MEXT of Japan. The authors are grateful to Dr. Mamoru Hashimoto from Osaka University for fruitful discussions.

[1] Th. Udem, R. Holzwarth, and T. W. Hänsch, Nature (London) **416**, 233 (2002).
[2] S. M. Foreman, D. J. Jones, and J. Ye, Opt. Lett. **28**, 370 (2003).
[3] F. Keilmann, C. Gohle, and R. Holzwarth, Opt. Lett. **29**, 1542 (2004).
[4] A. Schliesser, M. Brehm, F. Keilmann, and D. W. van der Weide, Opt. Express **13**, 9029 (2005).
[5] D. M. Mittleman, R. H. Jacobsen, R. Neelamani, R. G. Baraniuk, and M. C. Nuss, Appl. Phys. B: Lasers Opt. **67**, 379 (1998).
[6] K. Kawase, Y. Ogawa, Y. Watanabe, and H. Inoue, Opt. Express **11**, 2549 (2003).
[7] G. Markelz, A. Roitberg, and E. J. Heilweil, Chem. Phys. Lett. **320**, 42 (2000).
[8] K. Yamamoto, M. Yamaguchi, F. Miyamaru, M. Tani, M. Hangyo, T. Ikeda, A. Matushita, K. Koide, M. Tatsuno, and Y. Minami, Jpn. J. Appl. Phys., Part 2 **43**, L414 (2004).
[9] D. W. van der Weide, J. Murakowski, and F. Keilmann, IEEE Trans. Microwave Theory Tech. **MTT-48**, 740 (2000).
[10] T. Yasui, E. Saneyoshi, and T. Araki, Appl. Phys. Lett. **87**, 061101 (2005).
[11] C. Janke, M. Först, M. Nagel, H. Kurz, and A. Bartels, Opt. Lett. **30**, 1405 (2005).